JOURNAL OF AIRCRAFT
Vol. 42, No. 5, September–October 2005

Reliability-Based Wing Design Optimization Using Trust Region-Sequential Quadratic Programming Framework

Joongki Ahn,* Suwhan Kim,† and Jang-Hyuk Kwon‡
Korea Advanced Institute of Science and Technology, Daejon 305-701, Republic of Korea

The computational efficiency of the reliability-based design optimization(RBDO) can be a critical issue when high-fidelity simulation methods are used. An efficient RBDO framework is presented that utilizes a single-loop RBDO algorithm in which reliability analysis and optimization are conducted in a sequential manner by approximating the limit-state function. A further improvement in computational efficiency is achieved by applying the fixed sensitivity of the limit-state function to the reliability analysis and the equivalent deterministic constraint calculation. To guarantee the convergence of the single loop and the fixed sensitivity algorithm, a trust region-sequential quadratic programming RBDO strategy, is developed. The proposed framework validates low-fidelity approximation models in the trust region radius. The framework is examined by solving an analytical test problem to show that the proposed strategy has the computational efficiency over existing methods while maintaining accuracy. The proposed strategy is applied to a three-dimensional aerodynamic wing design problem to get improved results satisfying probabilistic constraints.

Introduction

RECENT studies have been conducted to consider uncertainty in the area of aerospace engineering.[1–5] In these studies, a airfoil and a three-dimensional flexible wing have been designed introducing geometrical uncertainties. They have used the first-order second-moment (FOSM) method to assess the effect of uncertainties. Even though FOSM is relatively easy to implement, it can not accurately predict the effect of uncertainty. It evaluates the constraint sensitivity only at the mean values of random input variables and uses only the normal distribution function. An advanced approach on uncertainty assessment is presented in Ref. 4, in which a design of a three-dimensional flexible wing under uncertainty is conducted. In the study, the probabilistic feasibility was searched by FOSM, and results of FOSM were compared with those of the first-order reliability method (FORM)[6,7] at the converged point. Because the FORM evaluates the sensitivity of constraint at the most probable point (MPP), it gives more accurate result than that of FOSM. The most recent work of the reliability-based design optimization using FORM is presented in Ref. 5. However, reliability analysis using FORM in design optimization is computationally expensive due to the required optimization problem within FORM. Therefore, the application of accurate reliability analysis methods to aerospace design problems has been still remained as a critical issue. Jang et al.[8] also point out the need for viable uncertainty-based design methods. For this reason, we propose an efficient reliability-based design optimization (RBDO) strategy, which can directly carry out the FORM analysis in design optimization.

The goal of RBDO is to find the best design that is sufficiently far from the failure region. RBDO is formulated as a nonlinear constrained optimization problem in which the constraint has a probabilistic form. Two types of difficulty exist in RBDO. The first one lies in calculating the probability of failure because the probabilistic constraint is a highly nonlinear function of the original deterministic function. This problem can be dealt with using approximate probability integration methods such as the FORM or the second-order reliability method (SORM). First the design is transform from the physical space to the normal space and then the limit-state function is approximate to compute the failure probability. FORM often provides adequate accuracy and is widely used for RBDO applications.

The other difficulty lies in the inherent double-loop structure of RBDO. In RBDO, the optimizer carries out a feasibility search in the outer loop, whereas the reliability analysis gives the probabilistic feasibility in the inner loop. Therefore, the inner loop for the reliability analysis is required at every outer loop cycle. This hampers the application of RBDO techniques to large-scale design problems such as computational fluid dynamics (CFD) and finite element method (FEM) simulations. Several alternative RBDO approaches have been studied to increase computational efficiency.[9–13] A single-loop–single-vector algorithm[9,10] linearizes the limit-state function to find the MPP. The safety-factor-based approach[11,12] and sequential optimization and the reliability assessment method[13] replace the probabilistic constraint to the equivalent deterministic constraint by shifting the boundary concept. It is assumed that the distance from the mean value to the MPP is fixed during the deterministic optimization. The constraints are calculated in the vicinity of the assumed MPP. Instead of calculating the probabilistic constraint, the equivalent deterministic constraint is used. The reliability analysis is separated from the optimization and arranged in a sequential manner. Thus, this is called a single-loop approach.[14] The reliability analysis and the optimization converge nicely and require fewer function evaluations than the traditional double-loop approach. The single-loop methods listed earlier have demonstrated have showed good capabilities in RBDO.

Based on the single-loop approach, we propose a fixed sensitivity strategy. It uses the same sensitivity in the reliability analysis and the deterministic constraint calculation. When that is done, there is no need for calculating expensive constraints in the deterministic optimization. However, the fixed sensitivity may not capture the nonlinear feature of the functions, which may cause convergence problems. To address the problem, optimization is performed under the trust region framework, which validates the approximated function at every cycle. Several approximation managements using trust region techniques have been developed.[15–18] One of the most promising aspects of the trust region method is its global convergence properties. It relies on the assumption that the approximated function and the original function match up to first order. In this study, the subproblem in the trust region framework has a sequential

Received 12 July 2004; revision received 28 October 2004; accepted for publication 30 November 2004.

*Ph.D. Student, Department of Aerospace Engineering.
†Doctoral Candidate, Department of Aerospace Engineering.
‡Professor, Department of Aerospace Engineering; jhkwon@kaist.ac.kr. Senior Member AIAA.

quadratic programming (SQP) form to exploit the advantages of the SQP. The trust region-SQP strategy allows the direct application of inequality constraints, and it exhibits second-order convergence near the solution. In addition to applying the trust region-SQP strategy, an algorithm to handle an infeasible starting point is implemented, in which the feasibility is enforced only for approximated constraints that are assumed to be infeasible. The algorithm rapidly drives the infeasible design point to the feasible region.

The paper is organized as follows. In the next section, traditional RBDO approaches are briefly reviewed. The proposed trust region-SQP framework is then described, with the concept of sharing an approximated function. A simple mathematical problem is tested to demonstrate the efficiency of proposed strategy. As an application, the result of three-dimensional wing design under uncertainty is presented. Finally, the paper concludes with the lesson learned and further work to be done.

Review of RBDO Approaches

The RBDO can generally be formulated as follows:

$$\underset{d}{\text{minimize}}\ f(\boldsymbol{d})$$

$$\text{subject to } P[g(\boldsymbol{x}) \geq 0] \leq \Phi(-\beta_t) \tag{1}$$

where $\boldsymbol{d} = \mu(\boldsymbol{x})$ is the design vector, that is, the mean value of the random vector $\boldsymbol{x}$. The probabilistic constraint is described by the limit-state function g, their probability distribution, and the reliability index β. A failure is defined when $g(\boldsymbol{x})$ is greater than 0. The probability of failure is the integration of the joint probability density function (PDF) $f_x(x)$ over the failure region,

$$p_f = \int_{g(x)<0} \cdots \int f_x(x)\,\mathrm{d}x \tag{2}$$

The direct computation of p_f by Eq. (2) is very difficult. In general, the information regarding the joint probability density $f_x(\boldsymbol{x})$ is lacking. Even if this information is available, the multiple integration is extremely complicated. Therefore, approximate probability integrations, such as FORM or SORM, have been developed to provide simplicity in computation. In FORM, probabilistic constraints in Eq. (1) can be expressed in two ways, reliability index approach (RIA) and performance measure approach (PMA).[19] PMA defines probabilistic constraints for a given β, whereas RIA defines the failure point where the limit-state function $g = 0$. Therefore, PMA is easier to solve than RIA due to simpler constraints with the fixed reliability index. The PMA formulation for probabilistic constraints is

$$\text{minimize } g(\boldsymbol{u})$$

$$\text{subject to } \|\boldsymbol{u}\| = \beta_t \tag{3}$$

where $\boldsymbol{u}$ is the standard normal random parameter that is transformed from the original random parameter $\boldsymbol{x}$. The optimum point on the given reliability surface is identified as the MPP. Equation (3) can easily be solved by the advanced mean value method (AMV) instead of nonlinear constraint optimization techniques. AMV iteratively updates the normalized direction vector of $\boldsymbol{u}$ to the steepest descent direction as can be seen in the following equation:

$$\boldsymbol{u}^{k+1} = \beta_t \cdot \alpha(\boldsymbol{u}^k) \tag{4}$$

where

$$\alpha(\boldsymbol{u}^k) = -\frac{\nabla_u g(\boldsymbol{u})}{\|\nabla_u g(\boldsymbol{u})\|}$$

The transformation from the standard normal space to the original space are related as follows:

$$\boldsymbol{x} = \boldsymbol{d} - \boldsymbol{u} \cdot \sigma_x \tag{5}$$

Although AMV associated with PMA can efficiently solve the probabilistic constraints in Eq. (1), double loops should be involved for optimization. Figure 1 is a flowchart for a conventional RBDO structure. Whenever the outer loop searches probabilistic feasibility, the inner loop should perform the reliability analysis in Eqs. (4) and (5). Thus, the computation can be prohibitive when expensive simulations, such as CFD or FEM, are associated with it.

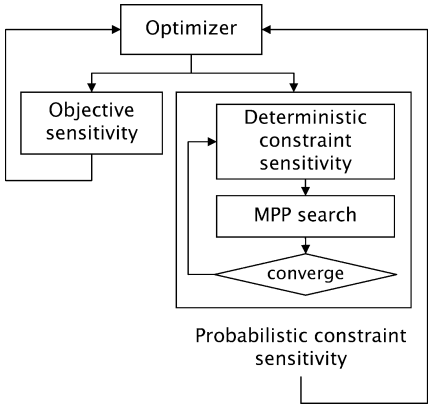

Fig. 1 Double-loop RBDO formulation.

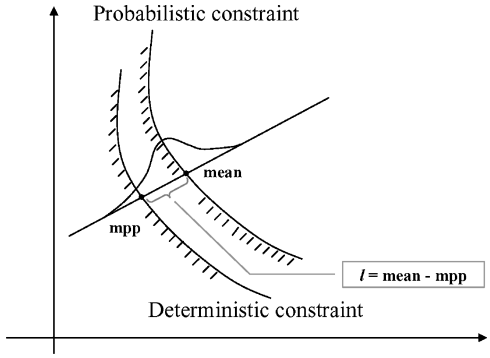

Fig. 2 Concept of shifting boundary.

To tackle the inefficiency of double-loop structure in RBDO, the optimization and reliability analysis are decoupled and arranged in a sequential manner. This is usually called a single-loop approach in which no reliability analysis is required within the optimization. Single-loop approaches are based on the fixed relation between the MPP and the mean point. The idea is that, when the probabilistic constraint in Eq. (1) is satisfied, the deterministic constraint can also be satisfied. Based on this concept, an equivalent deterministic constraint is introduced such that the probabilistic constraint is replaced by an equivalent deterministic one. The equivalent deterministic constraint is shown in Fig. 2. If we know the distance l from the mean point to the MPP by reliability analysis and assume that the distance is fixed along a small perturbation of the mean value, we can evaluate the constraint on the deterministic boundary instead of the probabilistic one. To correct the error caused by the assumption of fixed distance, the distance l is updated whenever the new MPP is obtained.

Sequential Approximation Management

Approximation of the Limit-State Function

The single-loop approach has been proven to be efficient in the literature. However, the approach requires calculation of expensive limit-state functions for the reliability analysis and for the equivalent deterministic constraints calculation at every iteration. This still hampers the use of computationally expensive simulations such as CFD and FEM analyses. To achieve better efficiency in RBDO, we implemented an approximation strategy for functions. The limit-state function is approximated as a linear function. The concept is similar to the single-loop single vector algorithm.[9,10] Because the conventional AMV in Eq. (4) has an iterative loop to correct the steepest descent gradient at current $\boldsymbol{u}$, the limit-state function should

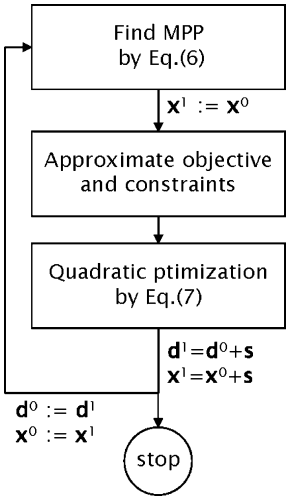

Fig. 3 Sequential approximation optimization flowchart.

be obtained for every iteration. Instead of calculating the gradient for every iteration, the fixed gradient at the previous MPP is used in Eq. (4). Therefore, no iteration loop is involved in the reliability analysis. The AMV with fixed gradient is given by

$$\boldsymbol{x} = \boldsymbol{d} + \beta_t \cdot \frac{\nabla_{u^0} g(\boldsymbol{u})}{\|\nabla_{u^0} g(\boldsymbol{u})\|} \cdot \sigma_x \tag{6}$$

where the superscript 0 refers to the point of previous MPP. The error caused by the linear approximation can be corrected as the mean values of design variables approach the optimum point. By the use of the fixed gradient of the limit-state function, little computation is required to find MPPs. To achieve further improvement in computational efficiency, the gradient of the limit-state function used at the previous reliability analysis is applied to the equivalent deterministic constraint. Hence, there is no need to calculate expensive constraints in the optimizer. The concept of using the same approximate function is based on the assumption that the distance from the mean point to the MPP is constant within a reliable move limit. In addition to approximating constraints, the objective function is also approximated to a quadratic model. Thus, the RBDO problem in Eq. (1) is replaced by the following equation:

$$\underset{s}{\text{minimize}} \ \nabla_{d^0} f^T \cdot \boldsymbol{s} + \tfrac{1}{2}\boldsymbol{s}^T B^0 \boldsymbol{s}$$

$$\text{subject to } g(\boldsymbol{x}^0) + \nabla_{x^0} \mathrm{g}^T \cdot \boldsymbol{s} \le 0 \tag{7}$$

where $\boldsymbol{s} = \boldsymbol{d} - \boldsymbol{d}^0$ and B^0 is the approximated Hessian obtained by the Broyden-Fletcher-Goldfarb-Shanno algorithm.

A flow chart of the reliability optimization with sequential approximation is shown in Fig. 3. The first step is finding the MPP $\boldsymbol{x}$ for each limit-state function by conducting an AMV analysis in Eq. (6). Because the gradient obtained at the previous MPP is used, no inner loop is required in the reliability analysis. After the MPP is found, the value and the gradient of the limit-state function are updated at the new MPP. The quadratic objective function is also updated using previous design values. The last step is solving the quadratic subproblem of Eq. (7).

Trust Region-SQP Framework

Even though the algorithm in Fig. 3 works well for many problems, it may have a convergence problem. Two kinds of error can be anticipated. The first one is caused by using the constant distance l between the mean value and the MPP. The other one is caused by using the same sensitivity of the limit-state function in the reliability analysis and the deterministic optimization. Because of errors, the reliability optimization procedure shown in Fig. 3 may not capture a nonlinear feature of the limit-state function. Therefore, the trust region strategy is introduced to validate the low-fidelity approximation in predicting the behavior of true models. The trust region method is an adaptive move limit strategy to improve the global behavior based on local models.

The quadratic subproblem in Eq. (7) makes it possible to apply the trust region-SQP method. The trust region-SQP method successively builds approximation models and minimizes nonlinear quadratic subproblems subject to trust region bounds and linear constraints. The trust region is tested to correct the size of trust region. The trust-region SQP method maintains the efficiency of SQP method of nonlinear optimization area. One of the properties of SQP is that it exhibits second-order convergence near the solution. It also can handle the inequality constraint directly instead of using the augmented Lagrangian form. By the addition of the trust region constraint in Eq. (7), a new model for trust region-SQP is given by

$$\underset{s}{\text{minimize}} \ \nabla_{d^0} f^T \cdot \boldsymbol{s} + \tfrac{1}{2}\boldsymbol{s}^T B^0 \boldsymbol{s}$$

$$\text{subject to } g(\boldsymbol{x}^0) + \nabla_{x^0} g^T \cdot \boldsymbol{s} \le 0$$

$$\|\boldsymbol{s}\| \le \triangle^t \tag{8}$$

The trust region test implies the success or failure of the current move limit. If the approximate functions predict the true model well, the trust region expands. On the other hands, it shrinks to increase accuracy. The test is measured by the ratio of the actual reduction in the merit function to that predicted by approximated merit function. The l_1 merit function is used because it is simple and inexpensive to evaluate. The true l_1 merit function is given by

$$\boldsymbol{\Phi}(\boldsymbol{d}; \boldsymbol{x}; \mu) = f(\boldsymbol{d}) + \rho \sum_{i \in E} |g_{E,i}(\boldsymbol{x})| + \rho \sum_{i \in I} \max[0, -|g_{I,i}(\boldsymbol{x})|] \tag{9}$$

where E and I are index sets of the equality and inequality constraints. The approximate merit function is modeled as follows:

$$\tilde{\boldsymbol{\Phi}}(\boldsymbol{d}; \boldsymbol{x}; \mu) = \tilde{f}(\boldsymbol{d}) + \rho \sum_{i \in E} |\widetilde{g_{E,i}}(\boldsymbol{x})| + \rho \sum_{i \in I} \max[0, -|\widetilde{g_{I,i}}(\boldsymbol{x})|] \tag{10}$$

To test the trust region, the reduction ratio r is introduced,

$$r = \frac{\Phi(\boldsymbol{d}^0; \boldsymbol{x}^0; \rho^0) - \Phi(\boldsymbol{d}^0 + \boldsymbol{s}; \boldsymbol{x}^1; \rho^0)}{\Phi(\boldsymbol{d}^0; \boldsymbol{x}^0; \rho^0) - \tilde{\Phi}(\boldsymbol{d}^0 + \boldsymbol{s}; \boldsymbol{x}^1; \rho^0)} \tag{11}$$

where superscripts 1 are current iteration indices and ρ is the penalty parameter. The closer r is to unity, the better the agreement is. The value of reduction ratio is increased or decreased depending on the quality of agreement. A good step occurs when the predicted reduction from the approximated merit function is close to the actual reduction experienced, for example, $r > 0.75$. A bad step occurs when, for example, $r > 0.25$, and the trust region radius would be decreased. The condition of the penalty parameter for global convergence and the practical updating algorithm are given in Ref. 20.

Unlike the trust region-augmented Lagrangian method, the trust region-SQP method usually encounters constraint inconsistency problems. When the feasible region of the linear constraints lies outside of the trust region, the subproblem in Eq. (8) can not find the solution in the trust region $\triangle^t$. The inconsistency is usually encountered in the trust region-SQP formulation. To resolve the problem, we present an algorithm in which the feasibility is enforced only for approximated constraints that are assumed to be infeasible. The subproblem to enforce feasibility is given by

$$\underset{s}{\text{minimize}} \sum_i \left[g_i(\boldsymbol{x}^1) + \nabla_{x^1} {g_i}^T \cdot \boldsymbol{s} \right]^+$$

$$\text{subject to } \|\boldsymbol{s}\| \le \triangle^t \tag{12}$$

where the notation is $[\tilde{g}]^+ = \max[0, \tilde{g}]$. The subproblem is invoked when the quadratic subproblem in Eq. (7) can not find a feasible solution. The computational cost of enforcing feasibility is also negligible because the optimization is based on the approximated functions.

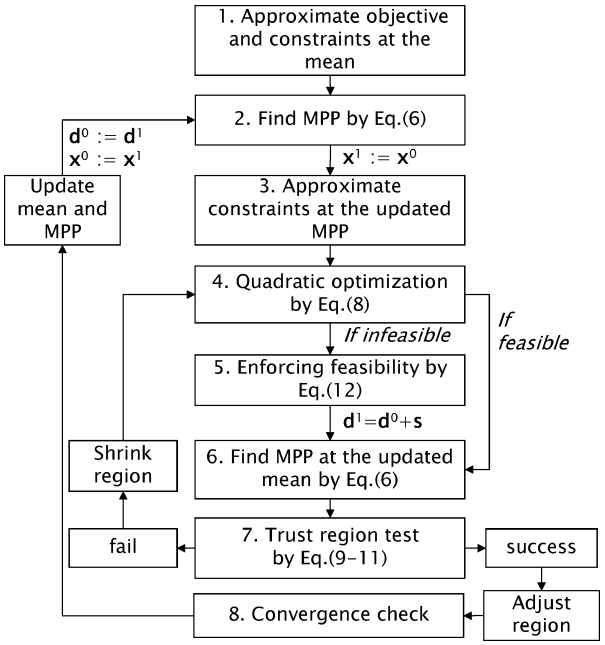

Fig. 4 Flow chart of trust region-SQP framework.

Figure 4 is a flowchart of the reliability optimization based on the trust region-SQP framework. The following steps describe the general procedure of the proposed method.

1) Approximate limit-state functions at initial MPPs. Usually the mean value is used as initial MPP.

2) Find MPPs using approximated limit-state functions by Eq. (6).

3) Approximate limit-state functions and objective functions at MPPs and at the mean point, respectively.

4) Solve the quadratic subproblem for $\boldsymbol{s} = \boldsymbol{d} - \boldsymbol{d}^0$ within the trust region radius $\triangle^t$. If the solution locates in the feasible region, update the mean value. Otherwise, go to step 5 to enforce feasibility.

5) Solve the linear subproblem for $\boldsymbol{s}$ to enforce the design to the feasible region. Update the mean value.

6) Find MPPs using the updated mean value by Eq. (6). Although, this step is not obligatory, it can improve the convergence property because MPPs are followed by the mean value.

7) Perform the ratio test by Eq. (10), and update the trust region radius. An example of updating the trust region radius and the design is as follows: If $r > 0.75$, then $\triangle^{t+1} = 2\triangle^t, \boldsymbol{d}^0 := \boldsymbol{d}^1, \boldsymbol{x}^0 := \boldsymbol{x}^1$. Else if $r < 0.25$, then $\triangle^{t+1} = 0.25\triangle^t, \boldsymbol{d}^0 := \boldsymbol{d}^0, \boldsymbol{x}^0 := \boldsymbol{x}^0$. Else $\triangle^{t+1} = \triangle^t, \boldsymbol{d}^0 := \boldsymbol{d}^1, \boldsymbol{x}^0 := \boldsymbol{x}^1$.

8) Return to step 2 until convergence. Check whether all of the design is feasible.

Applications

Test Problem

To validate the proposed framework, we use an analytical test problem taken from Ref. 19. It has three nonlinear constraints with two-dimensional random design variables: $\underset{d}{\text{minimize}}\ f = d_1 + d_2$ subject to

$$\mathrm{g}(1) = P\left(1 - \frac{(x_1+4)^2 + (x_2-3)^2}{50} \le 0\right) \le \Phi(\beta_t)$$

$$\mathrm{g}(2) = P\left(1 - \frac{10x_2^3 - x_1^2 x_2 - 2x_1}{10} \le 0\right) \le \Phi(\beta_t)$$

$$\mathrm{g}(3) = P\left(1 - \frac{80}{d_1^2 + 8x^2 + 5} \le 0\right) \le \Phi(\beta_t) \qquad (13)$$

where

$$\beta_t = -1.644, \qquad x_1 \sim N\left(d_1, 0.5^2\right), \qquad x_2 \sim N\left(d_2, 0.4^2\right)$$

Table 1 Results for test problem

$\boldsymbol{d}$[a]	$f(\boldsymbol{d})$	$g(\boldsymbol{x})$	Number of function evaluations
		Double loop	
3.8602		0.0000	462
	6.1547	0.0000	471
2.2945		−0.7048	561
		Single loop[13]	
3.8554		0.0000	162
	6.0999	0.3125	150
2.2444		−0.7211	156
		Trust region-SQP	
3.8602		0.0000	43
	6.1547	0.0000	43
2.2945		−0.7065	43

[a]Start point is feasible (5,5).

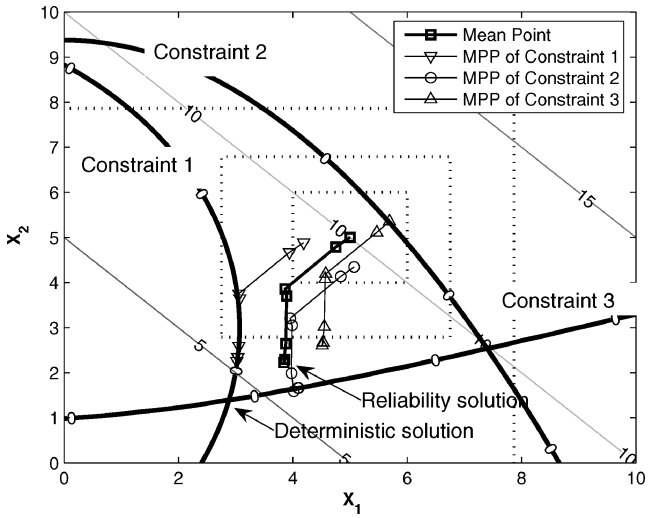

Fig. 5 Converging history with feasible starting point.

Random variables x_1 and x_2 are supposed to have normal distributions with means $\boldsymbol{d}$ and standard deviations of 0.5 and 0.4, respectively. The reliability index is given as -1.644 whose cumulative distribution function, denoted as Φ, approximately equals to 0.05 in standard normal distribution. Each constraint requires that the probability of failure should be less than 5%. The probability of failure means the probability that the value of each constraint is less than 0.

Figure 5 shows the solution space and converging history obtained by the trust region-SQP framework. The objective function is shown as contour lines whereas the three constraint boundaries are bold lines. The dotted rectangles are the trust region radi: used at each iteration. The converging history of mean values (squares) and MPPs are shown. Note that the MPP of each constraint follows the mean value with the fixed distance l as described in Fig. 2. At the converged point, constraints 1 and 2 are identified as active constraints because their MPPs lie on the constraint boundaries. The optimum mean value is kept apart from the deterministic constraint boundaries. The distance can be interpreted as a reliability margin under uncertainty of input variables. Table 1 lists results of the proposed method with those of existing methods for the test problem. All methods are tested by MATLAB® fmincon optimizer. The double-loop method and the proposed trust region-SQP give the same feasible solution whereas the single-loop algorithm[13] violates the second constraint. Although the convergence characteristics of the methods are different from each other, we can see that the proposed method resulted the least number of function evaluations while maintaining accuracy.

The infeasible starting point is also tested as shown in Fig. 6. At the starting point (1,4), constraint 1 is violated and the constraint boundary is out of the trust region. Therefore, the subproblem in Eq. (12) is invoked to enforce the design point to the feasible region. The feasibility enforcement algorithm is invoked only at the first

Table 2 List of design variables

Variable	μ	σ	Initial design[a]	PDF
Mach	0.84	0.003	0.84	Normal
AOA	3.06	0.02	3.06	Normal
Sweep	μ_{Sweep}	0.10	30.26	Normal
Taper	μ_{Taper}	0.02	0.56	Normal

[a]Initial design parameters are those of ONERA M6 wing.

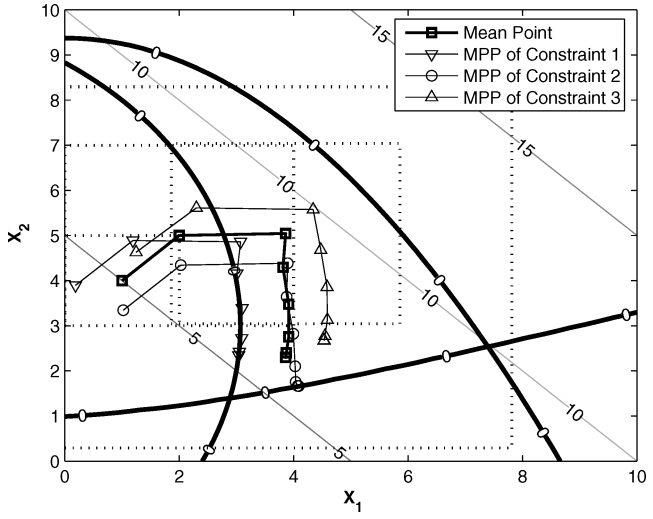

Fig. 6 Converging history with infeasible starting point.

iteration. At the second iteration, although the design locates in the infeasible region, the algorithm is not invoked because the trust region radius covers the constraint boundary.

Three-Dimensional Wing Design

With use of the proposed method, a three-dimensional aerodynamic wing is optimized considering uncertainty. The initial geometry for the three-dimensional wing is the the ONERA M6 wing. A compressible Euler code is used as the flow solver. The computational grid system is an O–H type with $129 \times 33 \times 33$ grid points. The analysis and optimization were conducted with different codes, FORTRAN for CFD analysis and MATLAB for reliability optimization. ModelCenter is used to integrate the two different codes. Uncertainties are categorized into operational uncertainty and geometrical uncertainty. Operational uncertainty contains the flight Mach number and the angle of attack (AOA) with constant mean values. The sweep angle and the taper ratio are selected as geometrical design variables. They can have uncertainties in the manufacturing process. The wing area is consistant with that of the ONERA M6 wing. If the number of random variables is large, the sensitivity of aerodynamic coefficients can be obtained from the adjoint method instead of the finite difference algorithm. However, we considered four random variables including two design variables for illustrative purpose. Table 2 summarizes variables used for the wing optimization.

The objective is maximizing the lift to drag ratio while satisfying probabilistic constraints. The first constraint in Eq. (14) states that the failure probability at lift coefficient of 0.35 should not be greater than -3σ. The second constraint can be stated in the same way. The values of the lift coefficient and pitching moment coefficient act as substitutes for vehicle weight and trim constraint, respectively,

$$\max(L/D)$$

$$\text{subject to} P(C_L \le 0.35) \le \Phi(-3)$$

$$P(|C_m| \le 0.28) \le \Phi(-3) \tag{14}$$

Figure 7 shows the design space and the converging history of mean design values and MPPs. Though the response of the objective function (lift to drag ratio) is not shown in Fig. 7, it increases as

Table 3 Comparison of results

Parameter	ONERA-M6	Deterministic design	Reliability-based design[a]
Sweep	30.26	38.63	35.87
Taper	0.56	0.4419	0.4420
L/D	19.6846	24.5748	21.9438
C_L	0.3620	0.35	0.3665
C_m	−0.2265	−0.28	−0.2665

[a]Results from the trust region-SQP framework.

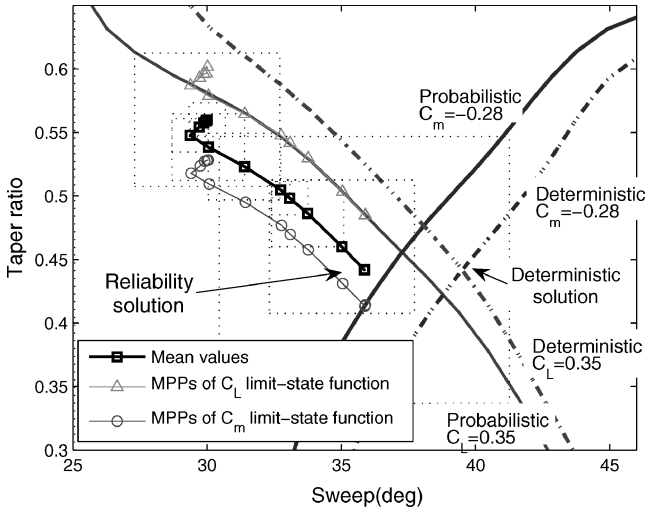

Fig. 7 Design space and converging history.

the sweepback angle increases and the taper ratio decreases. The lower right corner of Fig. 7 can have the maximum lift to drag ratio. Dash–dot lines represent the deterministic constraint boundaries of C_L and C_m. Therefore, the solution of deterministic optimization locates at the intersection of two deterministic constraints. The solid lines indicate probabilistic constraint boundaries obtained at converged MPP of the Mach number and the AOA. Note that deterministic constraints boundaries are moved to the left to be probabilistic boundaries, so that the area of the feasible region is decreased. The feasible region of the probabilistic constraints decreases compared to that of the deterministic constraints to consider uncertainties of the Mach number and the AOA. It can be seen that the converged reliability solution is apart from probabilistic constraint boundaries to ensure uncertainties of the sweep angle and the taper ratio.

Note that the probabilistic constraint of the lift coefficient is violated at the starting point. However, at the beginning, the feasibility enforcing step is not invoked because the initial trust region radius covers the constraint boundary. The initial trust region radius is set to 15% of the full design space. In the next iteration, the poor approximation of the constraint gives a negative value of the reduction ratio, which makes the trust region shrink. The constraint boundary locates out of the reduced trust region. In this case, the feasibility enforcing step is invoked in the course of the iterations.

In Table 3, results of the reliability optimization are compared with those of the original design and the deterministic optimization design. Although the lift to drag ratio of the reliability design has been increased from that of ONERA M6 wing, it is relatively smaller than that of the deterministic design. Introducing uncertainties into the design variables decreases the lift to drag ratio. The reliability of the system is in compensation for the loss of the lift to drag ratio. The seemingly small uncertainties produce substantial changes in the wing performance. Values of lift and pitching moment coefficients in the deterministic optimization are equal to 0.35 and −0.28, respectively. This means that, if uncertainties are involved, the deterministic design could fail. On the other hand, values of reliability design have small margins to consider uncertainties.

Table 4 Comparison of methods

Method	No. of function evaluations
Double loop	1182
Single loop[13]	428
Trust region-SQP	260

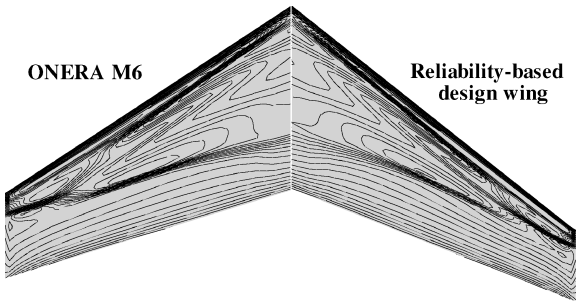

Fig. 8 Planform of ONERA M6 and reliability-based design wing.

The resulting planform shape can be readily seen in Fig. 8, which also shows the surface pressure contours of the original ONERA M6 wing and the reliability-based design one. It can be seen that the λ shocks still exist for both wings. This is the reason why airfoil surface parameters are not considered as design variables. Further research will be focused on considering uncertainties of the airfoil surface parameters.

Table 4 shows the computational efficiency of the proposed strategy. It compares the number of function evaluations until convergence reached. The computational efficiency of the trust region-SQP can be affected by many parameters such as the initial trust region radius, the value of penalty parameter, and adjusting trust region radius parameters. Moreover, the convergence characteristics are different from each other. Although the result in Table 4 shows a specific case, the computational efficiency did not vary much. Generally, the proposed method gives the superior efficiency to the other methods.

Conclusions

An efficient strategy for taking into account uncertainties has been presented. The strategy integrates FORM into the design optimization process to improve accuracy. The computational efficiency is a critical issue in RBDO when high-fidelity simulation methods are used. We utilize the concept of the single-loop RBDO algorithm. To improve computational efficiency, the approximated sensitivity of the limit state function is used in the deterministic constraint. The approximate functions are validated in the trust region-SQP framework, which yields a robust convergence characteristics.

The converged solution for the test problem showed good agreement with other methods. Substantial reduction in the computing cost is observed compared with the existing methods. A three-dimensional wing design optimization under uncertainties also demonstrates the efficiency of the proposed method. The converged solution yields improved aerodynamic performance and reliability.

References

[1]Huyse, L., and Lewis, R. M., "Aerodynamic Shape Optimizaton of Two-dimensional Airfoils Under Uncertain Conditions," NASA CR2001-210648, Jan. 2001.

[2]Pukto, M. M., Newman, P. A., Taylor, A. C., III, and Green, L. L., "Approach for Uncertainty Propagation and Robust Design in CFD Using Sensitivity Derivatives," AIAA Paper 2001-2528, June 2001.

[3]Gumbert, C. R., Newman, P. A., and Hou, G. J.-W., "Effect of Random Geometric Uncertainty on the Computational Design of a 3-D Flexible Wing," AIAA Paper 2002-2806, June 2002.

[4]Gumbert, C. R., Hou, G. J.-W., and Newman, P. A., "Reliabilty Assessment of a Robust Design Under Uncertainty for a 3-D Flexible Wing," AIAA Paper 2003-4094, June 2003.

[5]Allen, M., and Maute, K., "Reliability-Based Design Optimization of Aeroelastic Structures," AIAA Paper 2002-5560, Sept. 2002.

[6]Hasofer, A. M., and Lind, N. C., "Exact and Invariant Second-moment Code Format," *Journal of Engineering Mechanics*, Vol. 100, No. 1, 1974, pp. 111–121.

[7]Rackwitz, R., and Fiessler, B., "Structural Reliability Under Combined Random Load Sequences," *Computers and Structures*, Vol. 9, 1978, pp. 489–494.

[8]Jang, T. A., Hemsch, M. J., Hilburger, M. W., Luckring, J. M., Maghami, P., Padula, S. H., and Stroud, W. J., "Needs and Opportunities for Uncertainty-Based Multidisciplinary Design Methods for Aerospace Vehicles," NASA TM-2002-211462, July 2002.

[9]Chen, X., and Hasselman, T. K., and Neill, D. J., "Reliability Based Structural Design Optimization for Practical Applications," AIAA Paper 97-1403, April 1997.

[10]Wang, L., and Kodiyalam, S., "An Efficient Method for Probabilistic and Robust Design with Non-Normal Distributions," AIAA Paper 2002-1754, April 2002.

[11]Wu, Y.-T., and Wang, W., "Efficient Probabilistic Design by Converting Reliability Constraints to Approximately Equivalent Deterministic Constraints," *Journal of Integrated Design and Process Science*, Vol. 2, No. 4, 1998, pp. 13–21.

[12]Wu, Y.-T., Shin, Y., Sues, R., and Cesare, M., "Safety Factor Based Approach for Probability-Based Design Optimization," AIAA Paper 2001-1522, June 2001.

[13]Du, X., and Chen, W., "Sequential Optimization and Reliability Assessment Method for Efficient Probabilistic Design," *ASME Journal of Mechanical Design*, Vol. 126, No. 2, 2004, pp. 225–233.

[14]Yang, R. J., and Gu, L., "Experience with Approximate Reliability-Based Optimization Methods," *Structural Multidisciplinary Optimization*, Vol. 26, Nos. 1–2, 2003, pp. 152–159.

[15]Alexandrov, N. M., Dennis, J. E., Lewis, R. M., and Torczon, V., "A Trust Region Framework for Managing the Use of Approximation Models in Optimization," NASA CR-201745, Oct. 1997.

[16]Rodriguez, J. F., Renaud, J. E., and Watson, L. T., "Convergence of the Trust Region Augmented Lagrangian Methods Using Variable Fidelity Approximation Data," *Structural Optimization*, Vol. 15, Nos. 3–4, 1998, pp. 141–156.

[17]Rodriguez, J. F., Renaud, J. E., Wujek, B. A., and Tappeta, R. V., "Trust Region Model Management in Multidisciplinary Design Optimization," *Journal of Computational and Applied Mathematics*, Vol. 124, Nos. 1–2, 2000, pp. 139–154.

[18]Alexandrov, N. M., Lewis, R. M., Gumbert, C. R., Green, L. L., and Newman, P. A., "Optimization with Variable-Fidelity Models Applied to Wing Design," AIAA Paper 2000-0841, Jan. 2000.

[19]Youn, B. D., and Choi, K. K., "Hybrid Analysis Method for Reliability-Based Design Optimization," *Journal of Mechanical Design*, Vol. 125, No. 2, 2003, pp. 221–232.

[20]Nodedal, J., and Wright, S. J, *Numerical Optimization*, New York, Springer-Verlag, 1999, pp. 434–439.